Animal Conservation

ZSL LET'S WORK FOR WILDLIFE

Animal Conservation. Print ISSN 1367-9430

Genetic potential for disease resistance in critically endangered amphibians decimated by chytridiomycosis

T. A. Kosch[1], C. N. S. Silva[2], L. A. Brannelly[1,3], A. A. Roberts[1], Q. Lau[4], G. Marantelli[5], L. Berger[1] & L. F. Skerratt[1]

1 One Health Research Group, College of Public Health, Medical and Veterinary Sciences, James Cook University, Townsville, Qld, Australia
2 Centre for Sustainable Tropical Fisheries and Aquaculture, College of Science and Engineering, James Cook University, Townsville, Qld, Australia
3 Department of Biological Sciences, University of Pittsburgh, Pittsburgh, PA, USA
4 Department of Evolutionary Studies of Biosystems, Sokendai (The Graduate University for Advanced Studies), Hayama, Japan
5 Amphibian Research Centre, Pearcedale, Vic, Australia

Keywords
major histocompatibility complex; *Pseudophryne corroboree*; *Batrachochytrium dendrobatidis*; genetic association; immunogenetics; amphibian declines; chytridiomycosis; disease resistance.

Correspondence
Tiffany Kosch, James Cook University, Townsville, Qld 4811, Australia.
Email: tiffany.kosch@jcu.edu.au.

Editor: Jeff Johnson
Associate Editor: Sabrina Taylor

Received 06 March 2018; accepted 17 September 2018

doi:10.1111/acv.12459

Abstract

Hundreds of amphibian species have declined worldwide after the emergence of the amphibian fungal pathogen *Batrachochytrium dendrobatidis* (*Bd*). Despite captive breeding efforts, it is unlikely that wild populations for many species will be reestablished unless *Bd* resistance increases. We performed a *Bd*-challenge study in the functionally extinct southern corroboree frog *Pseudophryne corroboree* to investigate differences in *Bd* susceptibility among individuals and populations, identify genetic [major histocompatibility complex (MHC) class I] and genome-wide variants associated with *Bd* resistance, and measure genetic diversity and population genetic structure. We found three MHC variants and one MHC supertype associated with *Bd* infection load and survival along with a suggestively associated single nucleotide polymorphism. We also showed that genome-wide heterozygosity is associated with increased survival. Additionally, we found evidence of significant population structure among the four *P. corroboree* populations studied and high MHC genetic diversity. Our results indicate that there are immunogenetic differences among captive southern corroboree frogs; such differences could be manipulated to increase disease resistance and mitigate the significant threat of chytridiomycosis. These results demonstrate a potential long-term solution to chytridiomycosis that could include breeding more resistant individuals and returning them to the wild.

Introduction

The emergence of the amphibian fungal pathogen *Batrachochytrium dendrobatidis* (*Bd*) has driven many species to extinction (Skerratt *et al.*, 2007). Although the southern corroboree frog *Pseudophryne corroboree* survived the initial epidemic, it is one of the world's most threatened vertebrate species, with fewer than 50 individuals remaining in the wild (McFadden *et al.*, 2013). *P. corroboree* and many other *Bd*-susceptible species are dependent upon captive breeding and reintroduction programs for their continued survival (Scheele *et al.*, 2014). However, these programs are unlikely to be self-sustaining unless *Bd* resistance increases. Therefore, a more stable long-term approach might be to apply genetic manipulation methods (e.g. genetic rescue, marker-assisted selection, genomic selection and genetic engineering) to increase resilience to this major threat (Jannink, Lorenz & Iwata, 2010; Petersen, 2017; Novak, 2018). Recent advances in molecular genetics have enabled the development of methods that do not require a reference genome, such as genotyping-by-sequencing, for non-model species (Narum *et al.*, 2013), which will facilitate genetic manipulation in wildlife for the first time.

Before genetic manipulation methods can be applied, detailed genomic studies must be performed to establish basic information on *Bd* immunity, including measuring phenotypic and genetic variance, and identifying genes associated with *Bd* resistance. The major histocompatibility complex (MHC) gene region has received considerable attention in the context of *Bd* immunity, due to its critical role initiating adaptive immune responses to pathogens in vertebrates. The MHC consists of several different classes of molecules, including classical class I (MHC class IA), which predominantly present peptides derived from intracellular pathogens to cytotoxic T cells, and classical class II (MHC class IIB), which present extracellular peptides to

helper T cells (Bernatchez & Landry, 2003). Genetic polymorphism of the MHC peptide binding region (PBR) determines the repertoire of pathogens that individuals and populations can respond to, making it a good candidate marker for disease association studies and population viability estimates. MHC class IIB alleles, conformations, supertypes and heterozygosity have been associated with *Bd* resistance (Savage & Zamudio, 2011; Bataille *et al.*, 2015), but the role of MHC class IA has not yet been investigated. However, the intracellular life stages of *Bd* make it a likely target for MHC class IA presentation (Richmond *et al.*, 2009; Kosch *et al.*, 2017). Furthermore, evidence that southern corroboree frogs have high MHC class IA diversity and that selection is acting on this gene region suggests that it may play a role in *Bd* immunity in this species (Kosch *et al.*, 2017).

Although the association between the MHC and *Bd* immunity is well-supported, the contribution of this gene region in comparison to other genes cannot be fully understood unless genome-wide approaches are used to characterize the genetic architecture of this trait. Characterizing the genetic architecture (i.e. how many genes are involved and their effect size) of *Bd* resistance is fundamental to understanding how this trait evolves as well as for making predictions of the potential for populations to persist in the presence of *Bd*. One commonly used approach to identify the variants controlling phenotypic traits is genome-wide association studies (GWAS), using genome-wide single nucleotide polymorphism (SNP) data (Bush & Moore, 2012). Additionally, population differences in structure and genetic diversity (e.g. heterozygosity) can be also used to investigate the evolutionary potential of endangered species (Harrisson *et al.*, 2014). Genetic diversity is the basis for adaptation and is a major element for species conservation. Evidence of unexpectedly large differences in allele frequencies (i.e. outliers) among populations can be indicative of natural selection (Lewontin & Krakauer, 1973).

The ability of natural populations to evolve disease resistance by directional selection is a key component to conserving species threatened by emerging infectious diseases. This process is dependent on two factors: individual phenotypic variation and for those variations to have a genetic basis. The aim of this study was to assess how genetic factors are associated with *Bd* susceptibility in *P. corroboree*. We experimentally exposed *P. corroboree* to *Bd* to test if: (1) survival varies across infected individuals and populations; (2) genetic variation at MHC loci and/or SNPs associates with infection load and survival; and (3) MHC alleles and/or SNPs display signatures of selection. This is the first genetic study to investigate the association between chytridiomycosis resistance and MHC class IA, and the first to use a genome-wide approach to characterize the genetic architecture of this trait. Finally, we also analyzed the genetic structure and diversity of four founder populations of the captive assurance colony and characterized their evolutionary potential, providing crucial information for improving the success of the *P. corroboree* captive breeding program.

Materials and methods

Animal husbandry and experimental *Bd* exposures

P. corroboree were collected as eggs from the wild from four separate populations [Cool Plains (C) (n = 20), Jagumba (J) (n = 18), Manjar (M) (n = 22), Snakey Plains (S) (n = 16)] (for site map see Kosch *et al.*, 2017) in the summers of 2003–2007. Census data during this period indicate that the species was undergoing precipitous declines, as there were only 13 calling males recorded across all known sites in 2007 (Hunter *et al.*, 2009). Corroboree frogs were inoculated with a New South Wales strain of *Bd* (AbercrombieR-L.booroologensis-2009-LB1 passage number 11) (see Supporting Information Data S1 for detailed information). Frogs were inoculated with 1×10^6 zoospores (*Bd* treatment, n = 76; controls, n = 17), and *Bd* infection load was measured weekly until the end of the experiment by quantitative polymerase chain reaction (qPCR) analysis of skin swabs using previously described protocols and DNA extraction methods (Brannelly *et al.*, 2015*a*). Each qPCR analysis contained a positive and negative control, positive control standards of 100, 10, 1 and 0.1 zoospore equivalents (ZE), and one replicate of each sample (Skerratt *et al.*, 2011). Frogs were checked daily for general health and clinical signs of chytridiomycosis (Brannelly, Skerratt & Berger, 2015*b*) and were euthanized with an overdose of MS-222 bath in accordance with animal ethics guidelines if deemed morbid (typified by lethargy and a slow righting reflex). The animals used in this experiment were part of a larger study (e.g. Brannelly *et al.*, 2016; Kosch *et al.*, 2017).

Survival differences among populations, MHC genotypes and genome-wide SNP heterozygosities were analyzed by Cox Regression analysis using the survival package in R (Therneau, 2015). Infection loads were transformed and analyzed using mixed models with nlme in R (Pinheiro *et al.*, 2009). Constructed models included the explanatory (fixed) factors of week, population, week×population and days survived. ANOVA was used to evaluate which models best fit the data. All survivors that naturally cleared infection post-experiment re-entered the captive breeding program.

MHC class I genotyping

DNA was extracted from *P. corroboree* tissues (skin, muscle, kidney, toe clips) from the *Bd* treatment group and amplified by polymerase chain reaction (PCR) using MHC class IA exon 2 primers, which amplify the hypervariable α1 PBR domain (Kosch *et al.*, 2017). Cloning and sequencing methods are described in Supporting Information Data S1. Resulting sequences were analyzed with Geneious (v. 9.0.5, Biomatters Ltd, Auckland, New Zealand) and identified as alleles if: (1) BLAST results indicated they were MHC class IA sequences, (2) they did not include stop codons, and (3) they were present in more than one copy per individual and more than one independent PCR reaction. Alleles were named based upon MHC

nomenclature rules described in Klein *et al.* (1993), and were assigned to supertypes to explore their peptide binding repertoires (Lillie *et al.*, 2015). Supertype designation was performed by first aligning *P. corroboree* amino acid sequences with that of *Homo sapiens* (HLA-A; D32129.1). Next we extracted amino acid sequences from the 13 PBR pocket positions identified in previous studies (Supporting Information Fig. S1; Matsumura *et al.*, 1992; Lebrón *et al.*, 1998) using R. We then characterized the 13 sites for five physiochemical descriptor variables: z1 (hydrophobicity), z2 (steric bulk), z3 (polarity), z4 and z5 (electronic effects) (Sandberg *et al.*, 1998; Didinger *et al.*, 2017) and performed discriminant analysis of principle components (DAPC) with R package adegenet (Jombart, Devillard & Balloux, 2010) to define functional genetic clusters. Alleles were assigned to clusters by a *K*-means clustering algorithm by selecting the model with the lowest Bayesian information criterion.

We tested for recombination and selection in our alignment using tests executed on the Datamonkey server, MEGA7 and omegaMap 5.0 (Wilson & McVean, 2006; Delport *et al.*, 2010; Kumar, Stecher & Tamura, 2016). Evolutionary relationships among *P. corroboree* nucleotide sequences and other vertebrates were inferred by constructing Neighbor-Joining phylogenetic trees in MEGA7. Evolutionary distances were computed using the Kimura 2-parameter gamma distributed method (K2 + G) and tree node support was estimated via 500 bootstrap replicates (Felsenstein, 1985). We investigated population differences in MHC class IA diversity using: (1) the number of unique alleles per population (A_P); (2) the number of alleles per individual (A_I); (3) number of private alleles per population (P_A); (4) mean evolutionary distance between nucleotides (D_{NUC}) and mean amino acid (D_{AA}) variation with MEGA7; (5) the total number of MHC supertypes per population (S_P); and (6) the mean number of MHC supertypes per individual by population (S_I). Number of alleles (A_I) and supertypes (S_I) per individual were summarized with a generalized linear model (GLM) in R assuming a Poisson distribution to model the count data. One-way analysis of variance (ANOVA) in R was used to compare population evolutionary distances between nucleotides (D_{NUC}) and amino acids (D_{AA}). Generalized least squares (GLS) models were used instead of GLM when variances were unequal. Arlequin was used to estimate pairwise fixation index (F_{ST}), and population differentiation was based on variance of allele frequencies among populations (Excoffier & Lischer, 2010).

Genotype-phenotype association analysis

To investigate the genome-wide association with infection load and survival, all infected individuals ($n = 76$) were genotyped by Diversity Arrays Technology Sequencing (DArTseq, Canberra, ACT, Australia). This genotyping-by-sequencing method uses restriction enzyme digestion and hybridization-based sequencing technology implemented on an NGS platform to generate biallelic SNPs, in ~70 bp DArTseq™ sequences (Cruz, Kilian & Dierig, 2013). Initial sequence quality control, marker filtering (i.e. to remove invariant SNPs and sequences with >1 SNP), and genotype calling performed by DArTseq™ resulted in 7513 SNPs (methods described in Lal *et al.*, 2017). Further filtering (minor allele frequency of 2%, call rate 70%, duplicate removal) and data formatting was then performed with dartQC (https://github.com/esteinig/dartQC) resulting in 3489 SNPs. Final quality control and GWAS was performed in GenABEL (Aulchenko *et al.*, 2007) and RepeatABEL resulting in 3245 SNPs (Rönnegård *et al.*, 2016) (see Supporting Information Data S1). Coverage of the final SNP dataset ranged from 3.00 to 79.56*x* (mean = 4.51*x* ± 2.32 SD). We also excluded one individual in which the identity by state was >0.9. We evaluated Hardy–Weinberg equilibrium (HWE) independently for each population to remove SNPs with $P \leq 0.001$ in all four populations as this is typically used to identify genotyping errors (Teo *et al.*, 2007); however, no SNPs were removed during this step. To investigate the associations between SNPs and the phenotypic traits we ran a separate GWAS for each phenotypic trait, three in total: (1) maximum infection load (log transformed), (2) days survived (log transformed), and (3) infection load per week. To account for population structure in the fitted models above, we included principal components derived from the genomic kinship matrix as fixed factors. *P*-value significance thresholds were adjusted for multiple-hypothesis testing with the Bonferroni equation using two different alpha thresholds ($\alpha = 0.05$, significant, $P < 1.54e\text{-}05$; $\alpha = 1.0$, suggestive, $P < 3.08e\text{-}04$) (Clarke *et al.*, 2011). The top ten suggestive SNPs from each of the three GWAS were selected to facilitate SNP comparison across methods (e.g. days survived, infection load), and annotated by searching the NCBI non-redundant nucleotide database with the software package Blast2GO (Götz *et al.*, 2008).

Population genetic analyses

Population genetic variation and thus long-term evolutionary potential of *P. corroboree* populations were measured using several approaches. Mean allelic richness (A_R) was estimated using the R package PopGenReport (Adamack & Gruber, 2014); observed heterozygosity (H_O), expected heterozygosity (H_E) and inbreeding coefficient (F_{IS}) were estimated using the R package diveRsity (Keenan *et al.*, 2013); individual heterozygosities were calculated using the MHL() function in R, and pairwise F_{ST} values and an exact *G*-test were calculated using the software GenePop on the web (Rousset, 2008). Because frog clutch information was not retained after collection, full sibling relationships were inferred from SNP data with the programs ML-Relate and Colony (v. 2.0.6.2) (Kalinowski, Wagner & Taper, 2006; Jones & Wang, 2010). Outlier markers were identified using the PCAdapt R package (Luu, Bazin & Blum, 2017) with a Benjamini–Hochberg FDR (false discovery rate) control and the level of FDR was set to 0.01. Because outlier markers can be indicative of selection (e.g. for disease resistance), we compared the frequency of outliers among populations. Population structure was analyzed with the program STRUCTURE (Pritchard, Stephens & Donnelly, 2000) and by

DAPC using adegenet package in R (Jombart, 2008). See Supporting Information Data S1 for detailed methods.

Results

Survival and infection load over time

Population of origin had a significant impact on days survived (Fig. 1a) (Cox regression: $\chi^2_3 = 9.72$, $P = 0.0211$), with population M surviving on average 14.2 days longer than the other three populations. Five frogs in the *Bd*-inoculated group survived to the end of the experiment: four from population M (18.2%) and one from population C (5.0%). All *Bd*-inoculated frogs were *Bd* positive for at least 2 weeks during the experiment, and infection loads increased over time in all but the five survivors. The five frogs that survived either successfully cleared infection ($n = 4$) or maintained low infection (6.7 ZE, $n = 1$) through week 12 post-inoculation. All survivors naturally cleared infection post-experiment.

The overall infection loads increased dramatically in the first half of the experiment (slope = 0.835), and then plateaued in the second half (slope = −0.225) (Fig. 1b). Therefore, the dataset was subdivided into two datasets (early < 5.5 weeks and late > 5.5 weeks) before mixed effects modeling. Infection intensity did not differ among populations ($F_{3,47} = 0.507$, $P = 0.678$; $F_{3,54} = 1.540$, $P = 0.215$), but there was an interaction effect of population and week in the later dataset ($F_{3,124} = 3.156$, $P = 0.0272$) where the slope for population M was less steep due to lower infection loads (ANOVA, $F_{3,185} = 14.63$, $P = 1.371e\text{-}08$).

MHC diversity and evolution

>We identified 22 unique MHC class IA PBR alleles (Supporting Information Fig. S1) among the four *P. corroboree* populations (C, J, M, S), comprised of 14 previously described (GenBank accessions KX372221–KX372232 and KY072979–KY072985) and seven newly described alleles (accessions MH588677–MH588683). Total alleles per individual ranged from 2 to 10 (Supporting Information Table S2). There were no population differences in mean number of alleles per individual (A_I) (GLM, $\chi^2 = 3.852$, d.f. = 3, $P = 0.278$), mean evolutionary distance between nucleotide variants (D_{NUC}) (GLS, $F_{3,71} = 2.527$, $P = 0.0643$), or mean evolutionary distance between amino acid variants (D_{AA}) (GLS, $F_{3,71} = 1.877$, $P = 0.141$) (Table 1). Mean nucleotide and amino acid distances across populations ranged from 0.169 to 0.188 and 0.297 to 0.322, respectively. These values fall toward the higher end of the range of MHC class IA data in other anurans (including that from robust populations) (reviewed in Kosch *et al.*, 2017). The most common MHC allele, Psco-UA*9, was present in >70% of individuals across populations (range = 31.0–85.0%) (Supporting Information Table S2; Fig. 2b). Alleles Psco-UA*24 and Psco-UA*27 were unique to population C and alleles Psco-UA*18 and Psco-UA*19 were unique to population M. After controlling for multiple simultaneous comparisons, only one MHC class IA pairwise F_{ST} comparison was significant for the four populations (adjusted P value = 0.008; M × C; Supporting Information Table S9).

We found no evidence of recombination among MHC alleles. There was evidence of positive selection acting on codons of the putative PBR pocket sites ($dN/dS = 2.128$, $Z = 2.921$, $P = 0.002$), but no evidence of positive selection on the non-PBR pocket sites ($dN/dS = 0.590$, $Z = -1.702$, $P = 1.000$) or the entire MHC class IA region ($dN/dS = 0.693$, $Z = -0.027$, $P = 1.000$). A positive Tajima's D value on the entire alignment supports that balancing selection or sudden population contraction has occurred ($D = 1.09$). In total, omegaMap identified 11 codon sites displaying evidence of positive selection, of which seven aligned with codons of human HLA-A PBR pocket positions (Supporting Information Fig. S1; residues 1, 16, 26, 53, 56, 57 and 60).

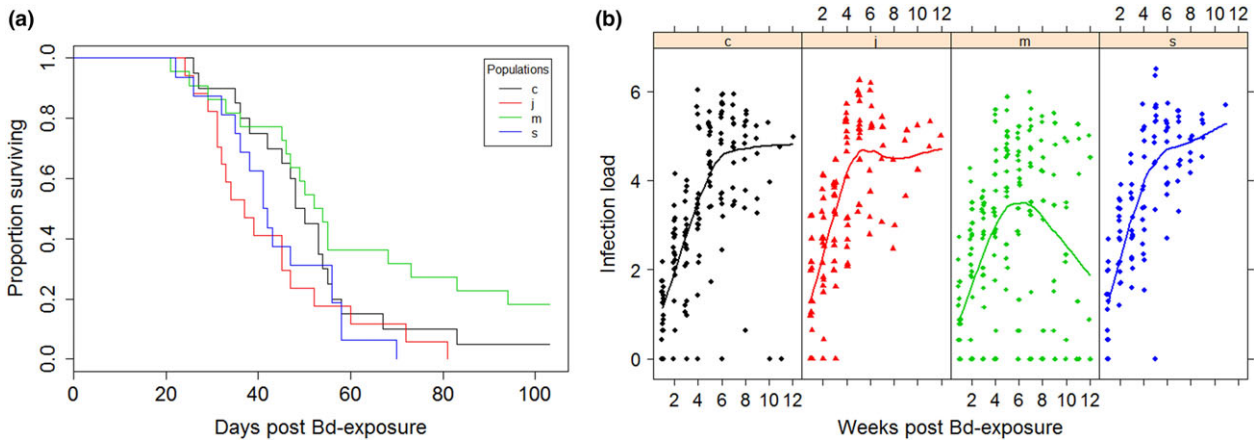

Figure 1 Interpopulation variation in *Batrachochytrium dendrobatidis* (*Bd*) infection load and mortality in laboratory exposed *Pseudophryne corroboree*. (a) Daily survivorship in *Bd* infected frogs. (b) *Bd* infection load [log10(ZE + 1)] over the course of the experiment as estimated by qPCR. Trend lines represent smooth fitted population means. Populations are represented by (c, black) Cool Plains, (j, red) Jagumba, (m, green) Manjar, and (s, blue) Snakey Plains.

Table 1 Major histocompatibility complex (MHC) class IA and single nucleotide polymorphism (SNP) diversity statistics by population

	Population			
	C	J	M	S
MHC				
N	20	18	22	16
A_P	17	17	20	14
A_I	5.75 (2.15)	5.72 (1.71)	6.41 (1.94)	4.88 (2.28)
P_A	2	0	2	0
D_{NUC}	0.187 (0.020)	0.169 (0.023)	0.183 (0.018)	0.188 (0.031)
D_{AA}	0.322 (0.038)	0.297 (0.034)	0.301 (0.029)	0.312 (0.038)
S_P	8	7	8	7
S_I	4.650 (1.387)	4.611 (1.420)	5.409 (1.469)	4.500 (1.789)
SNPs				
N	20	18	22	16
N_A	6888	6793	6900	6721
H_O	0.388	0.370	0.401	0.361
H_E	0.366	0.339	0.374	0.335
A_R	1.37	1.34	1.38	1.34
F_{IS}	−0.050	−0.073	−0.060	−0.065

Values in parenthesis representing the standard deviation.

C, Cool Plains; J, Jagumba; M, Manjar; S, Snakey Plains; N, number of individuals; A_P, total number of alleles per pop; A_I, number of alleles per individual averaged per population; P_A, private allele count; D_{NUC}, mean pairwise nucleotide diversity (*p*-distance); D_{AA}, mean pairwise amino acid diversity (*p*-distance); S_P, total number of supertypes per population; S_I, number of supertypes per individual averaged per population; N_A, number of SNP alleles; H_O, heterozygosity observed; H_E, heterozygosity expected; A_R, mean allelic richness; F_{IS}, inbreeding coefficient.

The 22 MHC alleles were allocated to eight distinct functional supertypes, each containing one to four alleles. The most common MHC supertype, ST8, was present in >80% of individuals (range = 68.0–90.0%) (Supporting Information Table S3; Fig. 2b). The number of supertypes per individual (S_I) ranged from 1 to 8 (mean = 4.83 ± 1.53 SD) with no difference among populations (GLM, $\chi^2 = 2.16$, d.f. = 3, $P = 0.541$).

Association analysis

Alleles Psco-UA*5 and Psco-UA*7 were positively associated with maximum infection load (Supporting Information Table S4; GLS, $F_{1,74} = 4.11$, $P = 0.0463$, $F_{1,74} = 10.56$, $P = 0.0017$). Allele Psco-UA*23 was negatively associated with number of days survived (Fig. 3; Supporting Information Table S6; GLS, $F_{1,74} = 12.96$, $P = 6e\text{-}04$). Alleles Psco-UA*5 and Psco-UA*7 were least common in the more resistant population M (23 and 14%, respectively) and most common in the susceptible population J (78 and 39%, respectively) (Supporting Information Table S2; Fig. 2a). Notably, only one of the five frogs that survived until the end of the experiment had a *Bd* susceptibility-associated allele (individual 18M, Psco-UA*5). Individuals with ST8 (comprised of alleles Psco-UA*5 and Psco-UA*5) had higher maximum infection loads than those with other STs (Supporting Information Table S6; GLS, $F_{1,74} = 4.49$, $P = 0.0374$) and a lower chance of survival (Fig. 3; Cox regression: $\chi^2_1 = 3.96$, $P = 0.04653$).

Our GWAS failed to reveal significant SNPs associated with *Bd* infection load and days survived (adjusted for multiple testing) (Supporting Information Fig. S4; Table S8). Low statistical significance of associated variants is typical of GWAS studies, especially when variant effect and sample sizes are small (e.g. Geng *et al.*, 2015); however, using less strict significance criteria or reporting top ranking variants could be an informative approach to explore possible variants that may influence focal traits. Several of the top SNPs were homologous to genes related to immune response and host reproduction, including pathogen recognition and control, and immune cell proliferation. Top SNPs associated with days survived included SNP 173 (homologous with the gene *RALGPS2*), and SNP 3440 (homologous to immunoglobulin Y) (Table 2 and Supporting Information Table S8). Two SNPs, SNP 1894 and SNP 1895, (homologous to Alpha-L-tissue fucosidase) overlapped across traits (maximum infection load and infection load per week).

SNP outliers and population structure

PCAdapt analyses with a FDR < 0.01 resulted in 3465 neutral and 24 outlier SNPs. There was no overlap between outlier SNPs and GWAS top suggestive SNPs; however, several SNP loci from these two methods were homologous to the Alpha-L-tissue fucosidase gene (Table 2).

F_{ST} values from all SNPs ranged from 0.106 to 0.191, F_{ST} values from neutral SNPs ranged from 0.105 to 0.188 and F_{ST} values from outliers ranged from 0.241 to 0.601 with populations M and J being the most differentiated and populations S and J being the least differentiated for all datasets (i.e. including all SNPs; Supporting Information

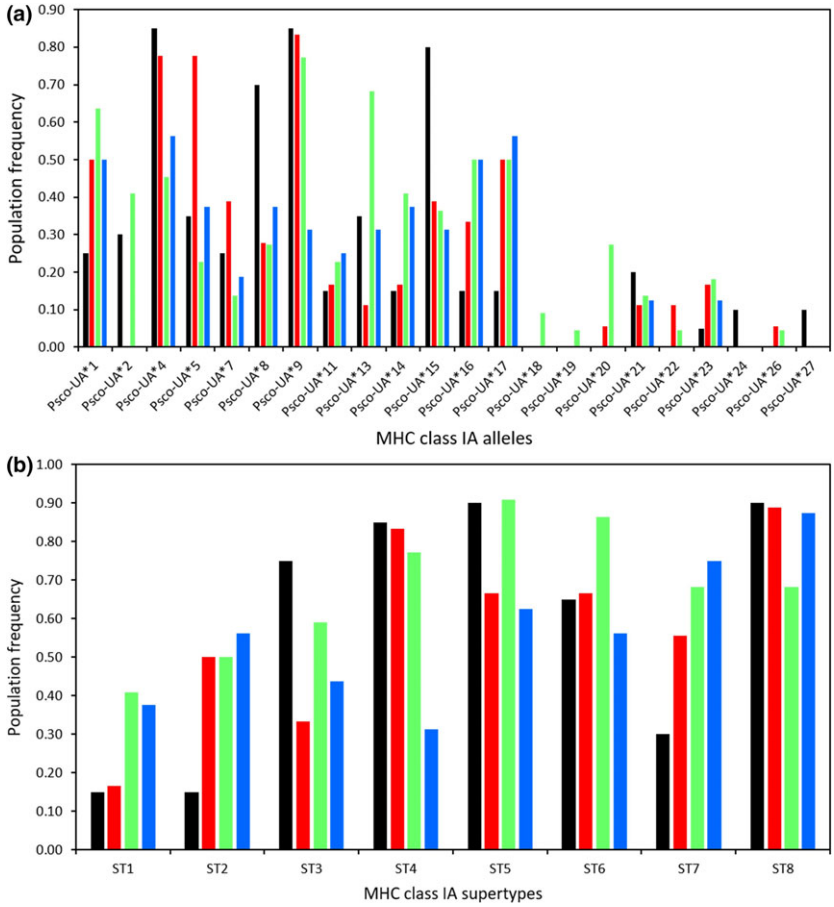

Figure 2 Major histocompatibility complex (MHC) class IA allele and supertype distributions among *Pseudophryne corroboree* populations. (a) allele and (b) supertype (ST) frequency distribution. (black) population C, (red) population J, (green) population M, and (blue) population S.

Table S9). DAPC plots using neutral SNPs showed all the populations clustering independently (Fig. 4a). When using only the 24 outlier SNPs, population M was distinctively separated from the remaining populations (Fig. 4b), which is likely due to the higher frequency of minor alleles in this population (Supporting Information Table S10). For both MHC class IA and SNP data, STRUCTURE analyses identified an optimum of two clusters ($K = 2$), with individuals separating into clusters following similar patterns to F_{ST} results (Supporting Information Table S9; Fig. S5). For MHC class IA, 85% of individuals from population C grouped into one cluster, while only 36.8% individuals from populations M and S grouped into the same cluster. For SNP data, population M was the most divergent from the other three populations (Supporting Information Table S9), which is in concordance with the DAPC results. Relationship assignments from ML-Relate and Colony provided similar results, identifying four to six full-sibling groups per population (Supporting Information Table S1).

Allelic richness values (A_R) ranged from 1.34 in populations J and S to 1.38 in population M. Negative inbreeding coefficients (F_{IS}) and observed heterozygosity (H_O) values greater than expected heterozygosity (H_E) in all populations indicate a deviation from HWE (Table 1). Individual genome-wide heterozygosity was positively associated with increased survival (Cox regression: $\chi^2_1 = 4.99$, $P = 0.03$). Additionally, *Bd* resistant population M had the highest levels of observed and expected heterozygosity, which aligns with evidence from other species correlating heterozygosity with fitness-related traits such as disease resistance (Harrisson *et al.*, 2014; Brock *et al.*, 2015).

Discussion

Our study demonstrates that southern corroboree frogs exhibit phenotypic and genetic variation associated with *Bd* susceptibility. We found that MHC alleles Psco-UA*5, Psco-UA*7, Psco-UA*23 and supertype 8 were associated with either increased *Bd* infection loads or lower survival times. We also identified a SNP that was suggestively correlated with *Bd* resistance (SNP 173), which is homologous with a gene (*RALGPS2*) that regulates immune cell proliferation. Diversity analyses indicate that despite recent declines, *P. corroboree* still contain high MHC class IA diversity. We also show that genome-wide heterozygosity is positively associated with *Bd* resistance at both the individual and

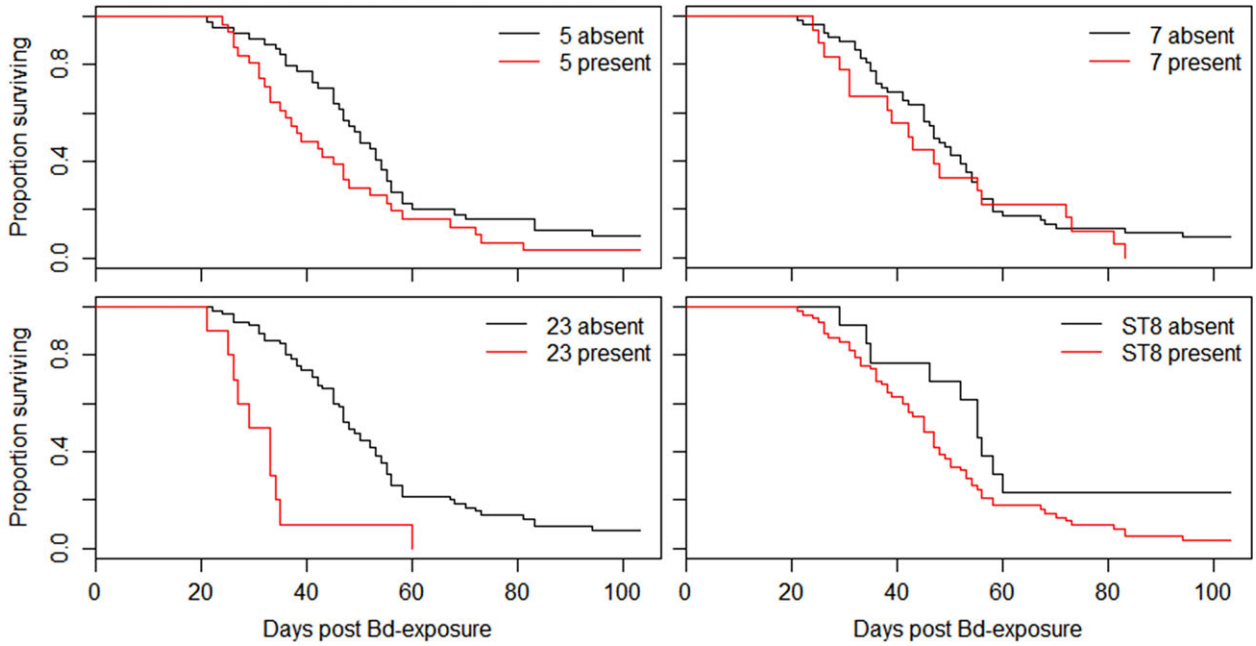

Figure 3 Impact of major histocompatibility complex class IA variants on *Pseudophryne corroboree* survival after *Batrachochytrium dendrobatidis* (*Bd*) exposure. (5) Psco-UA*5, (7) Psco-UA*7, (23) Psco-UA*23, (ST8) supertype 8. Allele Psco-UA*23 and supertype 8 were significantly associated with days survived. ST, supertype.

Table 2 Putative gene functions of notable top single nucleotide polymorphism (SNP) loci identified by genome-wide association studies (GWAS) and outlier analyses

SNP ID	Gene	Putative function	Method	*P*-value	References
34	Slc4a9	Sodium bicarbonate solute carrier	GWAS: Max	$5.10E^{-13}$	Lipovich *et al.* (2001)
173	Guanine nucleotide exchange factor	A molecular switch involved in cell differentiation and proliferation	GWAS: Days	$9.20E^{-05}$	Alberts *et al.* (2002)
1894, 1895, and 18 others	Alpha-L-tissue fucosidase	Cleaves fucose containing glycoproteins	GWAS and/or outliers	≤0.006	Nemanic *et al.* (1983), Takashima, Hamamoto & Nakase (2000)
3440	Immunoglobulin Y	Pathogen recognition and control	GWAS: Days	0.002	Warr, Magor & Higgins (1995), Ramsey *et al.* (2010), Young *et al.* (2014), Poorten *et al.* (2016), Fernández-Loras *et al.* (2017)
79	RAD51	Genetic recombination and DNA repair	Outlier	$6.42E^{-15}$	Maeshima, Morimatsu & Horii (1996), Yamamoto *et al.* (1999)
2794	ODF2	Maintains the elastic structure of sperm tails	Outlier	$3.68E^{-05}$	Petersen, Fuzesi & Hoyer-Fender (1999)
2603	Toll-like receptor 7	Pathogen recognition and innate immunity activation	Outlier	$1.50E^{-05}$	Van Prooyen *et al.* (2016)
759	Nrf3	Antioxidant response transcription factor	Outlier	$4.01E^{-07}$	Chevillard, Paquet & Blank (2011)
2174	Cab3	Regulatory subunit of the voltage-dependent calcium channel	Outlier	$1.36E^{-05}$	Bosch *et al.* (2003), Voyles *et al.* (2009)
928	ORP1 (OSBPL1A)	Multiple functions, including antigen processing and presentation	GWAS: Days	$6.80E^{-04}$	Rocha & Neefjes (2008), van den Hoorn *et al.* (2011)

P-values are unadjusted, Bonferroni adjusted alpha significance thresholds ($\alpha = 0.05$, significant, $P < 1.54e\text{-}05$; $\alpha = 1.0$, suggestive, $P < 3.08e\text{-}04$).

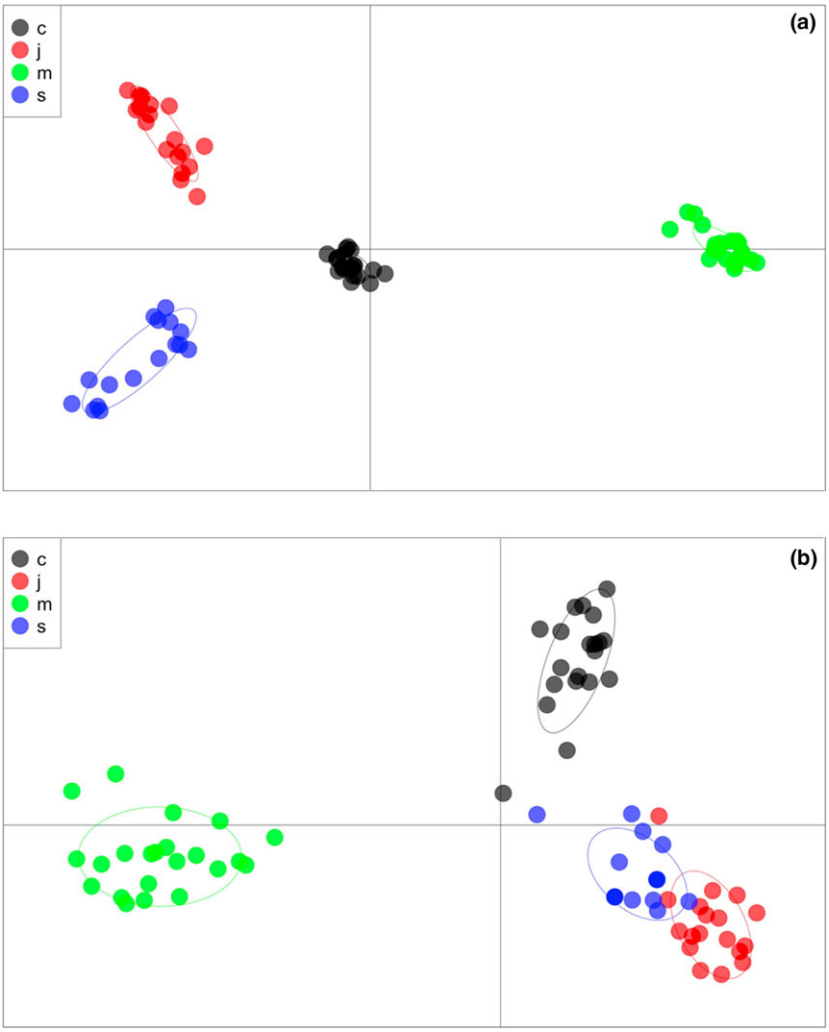

Figure 4 Discriminate analysis of principal components using 3465 neutral single nucleotide polymorphisms (SNPs) (a) and 24 outlier SNPs (b).

population level, indicating that genetic diversity may play a role in *Bd* resistance. Additionally, we provide evidence of significant population structure among the four *P. corroboree* populations, which confirms natural history observations for this species of low vagility. Evaluating genetic diversity and understanding the genomic basis of disease susceptibility in wildlife is critical to managing declining populations. Genome-wide and candidate gene association approaches such as those applied here have begun to identify genetic variants associated with immunity in threatened species such as gopher tortoises, Tasmanian devils and little brown bats (Donaldson *et al.*, 2017; Wright *et al.*, 2017; Elbers, Brown & Taylor, 2018). Once identified, variants associated with disease resistance can be manipulated to increase population persistence in the presence of threats such as *Bd*.

We found that *P. corroboree* exhibit phenotypic variation in resistance to *Bd* infection at the population level. This was evident in both the days survived and infection load through time. One population (M) was distinct from the other three populations by having the longest survival, lowest infection loads and most individuals that survived until the end of the experiment. Phenotypic differences in *Bd* resistance were associated with genetic variance of the MHC. Three MHC alleles and one MHC supertype were associated with increased *Bd* susceptibility in individual frogs. Notably, only one of the five survivors had a *Bd* susceptibility-associated MHC allele. Susceptibility variants may increase disease susceptibility by lowering the binding affinity of MHC class I molecules for *Bd* peptides. This mechanism has been suggested for MHC class II in other frogs (Bataille *et al.*, 2015), but has yet to be investigated using functional approaches like MHC binding affinity assays, as are commonly applied in humans and model species (e.g. Harndahl *et al.*, 2009; Goulder & Walker, 2012).

Our GWAS did not identify any SNPs that were significantly associated with *Bd* resistance, which may be the result of the limited sample size of this pilot study combined with the potential polygenic nature of the traits analyzed here (see

Supporting Information Data S1 on GWAS limitations). One SNP that was suggestively negatively associated with days survived (173) had closest homology to the *RALGPS2* gene of *Xenopus tropicalis.* This gene might influence *Bd* outcomes by regulating the proliferation of cells critical to *Bd* immunity such epidermal or immune cells (Ellison *et al.*, 2014). Another top SNP (3440) was homologous to immunoglobulin Y (IgY). The contribution of IgY to *Bd* immunity varies across species. *X. laevis* immunized against *Bd* produced a strong pathogen-specific IgY response (Ramsey *et al.*, 2010), whereas IgY response is suppressed or unaffected during *Bd* infection in other species (Young *et al.*, 2014; Poorten *et al.*, 2016).

Tests of selection indicated that codons of the putative MHC PBR pockets are under putatively positive selection in *P. corroboree*, suggesting that these amino acid residues could provide a survival advantage to *Bd* infected hosts. Even though we did not detect any MHC alleles associated with *Bd* resistance, our finding of three MHC class IA alleles and one supertype associated with higher susceptibility supports that *P. corroboree* MHC has a functional role in *Bd* immunity. In other frog species, MHC class IIB alleles and supertypes have been correlated with increased *Bd* resistance (e.g. Savage & Zamudio, 2011) likely due to higher binding affinity for *Bd* peptides. This correlation is also probable for MHC class IA, as has been demonstrated in pathogen systems of other species (Madsen & Ujvari, 2006; Aguilar *et al.*, 2016).

Of the 24 SNPs that were putatively adaptive (i.e. population outliers), there are several that might play a role in the evolution of *Bd* resistance in *P. corroboree* due to their homology to genes that influence pathogen response or reproduction in other species. SNP 2603 has homology to toll-like receptor 7, which is involved in pathogen recognition and activation of innate immunity in other species (e.g. Van Prooyen *et al.*, 2016), and therefore may also be involved in the response of frogs to *Bd* infection. Other relevant adaptive SNPs include those that may act in response to *Bd*-induced effects on hematopoietic tissue, electrolyte transport and cardiac function (Voyles *et al.*, 2009; Brannelly *et al.*, 2016).

Several SNP loci identified from our GWAS and outlier analyses were homologous to the Alpha-L-tissue fucosidase gene. Fucosidases remove cell surface fucose residues, and are likely involved in mammalian epidermal differentiation from the stratum granulosum to stratum corneum (Nemanic, Whitehead & Elias, 1983). The association of a fucosidase gene with infection load is supported by the observed thickening of the amphibian stratum corneum during chytridiomycosis pathogenesis (Berger *et al.*, 1998). Fucose is also a prominent component of the amphibian skin mucus where it may play a role in innate immunity by inhibiting pathogen adhesion to epidermal cells (Meyer *et al.*, 2007). Interestingly, *Bd* zoospores have been shown to exhibit positive chemotaxis to this compound (Van Rooij *et al.*, 2015), suggesting that host regulation of fucosidase gene expression may influence *Bd* infection.

Southern corroboree frog populations showed significant evidence of genetic structure among all four populations studied, with population M being the most differentiated in pairwise F_{ST} comparisons across all datasets, and populations J and S were the least differentiated. The population divergence estimates for this species are consistent with their life history and microsatellite data, which indicates that interbreeding among populations separated by even a few km is low (Morgan *et al.*, 2008). Low interbreeding rates, along with low fecundity and low reproduction rates, have likely contributed to the demise of *P. corroboree* after the introduction of *Bd*; despite evidence of *Bd* resistance in some individuals as genetic variants related to *Bd* resistance are unlikely to spread. This contrasts species that are persisting with *Bd*, which have adapted higher recruitment rates and rapid turnover in response to the pathogen (e.g. *Litoria verreauxii alpina*, Scheele *et al.*, 2017; *L. rheocola*, Phillott *et al.*, 2013).

Concluding remarks and future directions

Southern corroboree frog populations have phenotypic and genetic variation in *Bd* susceptibility, and therefore have the potential to be genetically manipulated to increase *Bd* resistance. Evidence of significant population structure suggests that this species may have declined, despite evidence of *Bd* resistance within some individuals, because genetic variants related to *Bd* resistance are unlikely to spread across the landscape if interbreeding rates are low. We show that despite functional extinction in the wild, MHC data indicate there is substantial genetic variation within the captive assurance collection. Our pilot study is a first step toward using genomic approaches to investigate polygenic immunity to *Bd* – a necessary step toward improving *Bd* resistance in susceptible species. Future studies should further examine the role that these identified SNPs and MHC variants play in *Bd* resistance. This could be investigated using genetic manipulation approaches (e.g. genomic selection, genetic engineering) to study gene function and modify phenotypes (Scheele *et al.*, 2014; Garner *et al.*, 2016; Johnson *et al.*, 2016). The feasibility of genetically manipulating wildlife to increase disease resistance has yet to be tested, but success in other systems (e.g. agriculture, model organisms) suggests that it is possible. The main challenge is accurately characterizing the heritability and genetic architecture of disease resistance as it requires many individuals to be studied (>1000) and better genomic resources (e.g. high-resolution SNPs, reference genomes).

Acknowledgments

We are grateful to C. Storlie, R. Jones, D. McKnight, and the JCU eResearch team for providing R scripting and statistical assistance, R. Webb, J. Hawkes, K. Fossen and C.D. Jong for assistance with animal husbandry, S. Bell for disease testing assistance, D. Hunter for conservation agency support, M. McFadden, P. Harlow, and R. Hobbs for animal husbandry advice, and K. Zenger, J. Eimes and A. Husby for discussion of analysis approaches. The research was supported by the

Australian Research Council grants (LP110200240; FT100100375), NSW-OEH, Taronga Zoo, experiment.com grant ('Can we stop amphibian extinction by increasing immunity to the frog chytrid fungus'), and Queensland Information Technology and Innovation Accelerate Fellowship Grant (14-218).

Data accessibility

MHC class IA DNA sequence data are available on GenBank (accessions MH588677–MH588683). The data generated from this study is accessible on Mendeley Data https://doi.org/10.17632/dwy4w2b8mv.1.

References

Adamack, A.T. & Gruber, B. (2014). PopGenReport: simplifying basic population genetic analyses in R. *Methods Ecol. Evol.* **5**, 384.

Aguilar, J.R.-D., Westerdahl, H., Puente, J.M.-D., Tomás, G., Martínez, J. & Merino, S. (2016). MHC-I provides both quantitative resistance and susceptibility to blood parasites in blue tits in the wild. *J. Avian Biol.* **47**, 669.

Alberts, B., Johnson, A., Lewis, J., Walter, P., Raff, M. & Roberts, K. (2002). *Molecular biology of the cell*. International Student Edition. 4th edn. New York: Garland Science.

Aulchenko, Y.S., Ripke, S., Isaacs, A. & Van Duijn, C.M. (2007). GenABEL: an R library for genome-wide association analysis. *Bioinformatics* **23**, 1294.

Bataille, A., Cashins, S.D., Grogan, L., Skerratt, L.F., Hunter, D., McFadden, M., Scheele, B., Brannelly, L.A., Macris, A. & Harlow, P.S. (2015). Susceptibility of amphibians to chytridiomycosis is associated with MHC class II conformation. *Proc. R. Soc. Lond. B Biol. Sci.* **282**, 20143127.

Berger, L., Speare, R., Daszak, P., Green, D.E., Cunningham, A.A., Goggin, C.L., Slocombe, R., Ragan, M.A., Hyatt, A.D., McDonald, K.R., Hines, H.B., Lips, K.R., Marantelli, G. & Parkes, H. (1998). Chytridiomycosis causes amphibian mortality associated with population declines in the rain forests of Australia and Central America. *Proc. Natl Acad. Sci. USA* **95**, 9031.

Bernatchez, L. & Landry, C. (2003). MHC studies in nonmodel vertebrates: what have we learned about natural selection in 15 years? *J. Evol. Biol.* **16**, 363.

Bosch, R.F., Scherer, C.R., Rüb, N., Wöhrl, S., Steinmeyer, K., Haase, H., Busch, A.E., Seipel, L. & Kühlkamp, V. (2003). Molecular mechanisms of early electrical remodeling: transcriptional downregulation of ion channel subunits reduces I Ca, L and I to in rapid atrial pacing in rabbits. *J. Am. Coll. Cardiol.* **41**, 858.

Brannelly, L.A., Berger, L., Marrantelli, G. & Skerratt, L.F. (2015*a*). Low humidity is a failed treatment option for chytridiomycosis in the critically endangered southern corroboree frog. *Wildl. Res.* **42**, 44.

Brannelly, L.A., Skerratt, L.F. & Berger, L. (2015*b*). Treatment trial of clinically ill corroboree frogs with chytridiomycosis with two triazole antifungals and electrolyte therapy. *Vet. Res. Commun.* **39**, 179.

Brannelly, L.A., Webb, R.J., Skerratt, L.F. & Berger, L. (2016). Effects of chytridiomycosis on hematopoietic tissue in the spleen, kidney and bone marrow in three diverse amphibian species. *Pathog. Dis.* **74**, pii: ftw069.

Brock, P.M., Goodman, S.J., Hall, A.J., Cruz, M. & Acevedo-Whitehouse, K. (2015). Context-dependent associations between heterozygosity and immune variation in a wild carnivore. *BMC Evol. Biol.* **15**, 242.

Bush, W.S. & Moore, J.H. (2012). Genome-wide association studies. *PLoS Comput. Biol.* **8**, e1002822.

Chevillard, G., Paquet, M. & Blank, V. (2011). Nfe2 l3 (Nrf3) deficiency predisposes mice to T-cell lymphoblastic lymphoma. *Blood* **117**, 2005.

Clarke, G.M., Anderson, C.A., Pettersson, F.H., Cardon, L.R., Morris, A.P. & Zondervan, K.T. (2011). Basic statistical analysis in genetic case-control studies. *Nat. Protoc.* **6**, 121.

Cruz, V.M., Kilian, A. & Dierig, D.A. (2013). Development of DArT marker platforms and genetic diversity assessment of the U.S. collection of the new oilseed crop *Lesquerella* and related species. *PLoS ONE* **8**, e64062.

Delport, W., Poon, A.F., Frost, S.D. & Pond, S.L.K. (2010). Datamonkey 2010: a suite of phylogenetic analysis tools for evolutionary biology. *Bioinformatics* **26**, 2455.

Didinger, C., Eimes, J.A., Lillie, M. & Waldman, B. (2017). Multiple major histocompatibility complex class I genes in Asian anurans: ontogeny and phylogeny of expression. *Dev. Comp. Immunol.* **70**, 69.

Donaldson, M.E., Davy, C.M., Willis, C.K., McBurney, S., Park, A. & Kyle, C.J. (2017). Profiling the immunome of little brown myotis provides a yardstick for measuring the genetic response to white-nose syndrome. *Evol. Appl.* **10**, 1076.

Elbers, J.P., Brown, M.B. & Taylor, S.S. (2018). Identifying genome-wide immune gene variation underlying infectious disease in wildlife populations–a next generation sequencing approach in the gopher tortoise. *BMC Genom.* **19**, 64.

Ellison, A.R., Savage, A.E., DiRenzo, G.V., Langhammer, P., Lips, K.R. & Zamudio, K.R. (2014). Fighting a losing battle: vigorous immune response countered by pathogen suppression of host defenses in the chytridiomycosis-susceptible frog *Atelopus zeteki*. *Genes Genomes Genetics* **4**, 1275.

Excoffier, L. & Lischer, H.E. (2010). Arlequin suite ver 3.5: a new series of programs to perform population genetics analyses under Linux and windows. *Mol. Ecol. Resour.* **10**, 564.

Felsenstein, J. (1985). Confidence limits on phylogenies: an approach using the bootstrap. *Evolution* **39**, 783.

Fernández-Loras, A., Fernández-Beaskoetxea, S., Arriero, E., Fisher, M.C. & Bosch, J. (2017). Early exposure to *Batrachochytrium dendrobatidis* causes profound immunosuppression in amphibians. *Eur. J. Wildl. Res.* **63**, 99.

Garner, T.W.J., Schmidt, B.R., Martel, A., Pasmans, F., Muths, E., Cunningham, A.A., Weldon, C., Fisher, M.C. & Bosch, J. (2016). Mitigating amphibian chytridiomycoses in nature. *Philos. Trans. R. Soc. Lond. B Biol. Sci.* **371**, 20160207.

Geng, X., Sha, J., Liu, S., Bao, L., Zhang, J., Wang, R., Yao, J., Li, C., Feng, J. & Sun, F. (2015). A genome-wide association study in catfish reveals the presence of functional hubs of related genes within QTLs for columnaris disease resistance. *BMC Genom.* **16**, 196.

Götz, S., García-Gómez, J.M., Terol, J., Williams, T.D., Nagaraj, S.H., Nueda, M.J., Robles, M., Talón, M., Dopazo, J. & Conesa, A. (2008). High-throughput functional annotation and data mining with the Blast2GO suite. *Nucleic Acids Res.* **36**, 3420.

Goulder, P.J. & Walker, B.D. (2012). HIV and HLA class I: an evolving relationship. *Immunity* **37**, 426.

Harndahl, M., Justesen, S., Lamberth, K., Røder, G., Nielsen, M. & Buus, S. (2009). Peptide binding to HLA class I molecules: homogenous, high-throughput screening, and affinity assays. *J. Biomol. Screen.* **14**, 173.

Harrisson, K.A., Pavlova, A., Telonis-Scott, M. & Sunnucks, P. (2014). Using genomics to characterize evolutionary potential for conservation of wild populations. *Evol. Appl.* **7**, 1008.

van den Hoorn, T., Paul, P., Jongsma, M.L.M. & Neefjes, J. (2011). Routes to manipulate MHC class II antigen presentation. *Curr. Opin. Immunol.* **23**, 88.

Hunter, D., Pietsch, R., Marantelli, G., McFadden, M. & Harlow, P. (2009). *Field research, recovery actions, and recommendations for the southern corroboree frog (Pseudophryne corroboree*) recovery program: 2007–2009. Sydney: Murray Catchment Management Authority.

Jannink, J.-L., Lorenz, A.J. & Iwata, H. (2010). Genomic selection in plant breeding: from theory to practice. *Brief. Funct. Genomics* **9**, 166.

Johnson, J., Altwegg, R., Evans, D., Ewen, J., Gordon, I., Pettorelli, N. & Young, J. (2016). Is there a future for genome-editing technologies in conservation? *Anim. Conserv.* **19**, 97.

Jombart, T. (2008). adegenet: a R package for the multivariate analysis of genetic markers. *Bioinformatics* **24**, 1403.

Jombart, T., Devillard, S. & Balloux, F. (2010). Discriminant analysis of principal components: a new method for the analysis of genetically structured populations. *BMC Genet.* **11**, 94.

Jones, O.R. & Wang, J. (2010). COLONY: a program for parentage and sibship inference from multilocus genotype data. *Mol. Ecol. Resour.* **10**, 551.

Kalinowski, S.T., Wagner, A.P. & Taper, M.L. (2006). ML-relate: a computer program for maximum likelihood estimation of relatedness and relationship. *Mol. Ecol. Notes* **6**, 576.

Keenan, K., McGinnity, P., Cross, T.F., Crozier, W.W. & Prodöhl, P.A. (2013). diveRsity: an R package for the estimation and exploration of population genetics parameters and their associated errors. *Methods Ecol. Evol.* **4**, 782.

Klein, J., Bontrop, R.E., Dawkins, R.L., Erlich, H.A., Gyllensten, U.B., Heise, E.R., Jones, P.P., Parham, P., Wakeland, E.K. & Watkins, D.I. (1993). Nomenclature for the major histocompatibility complexes of different species: a proposal. In *The HLA system in clinical transplantation*: 407–411. Solheim, B.G., Ferrone, S. & Möller, E. (Eds). Heidelberg: Springer.

Kosch, T.A., Eimes, J.A., Didinger, C., Brannelly, L.A., Waldman, B., Berger, L. & Skerratt, L.F. (2017). Characterization of MHC class IA in the endangered southern corroboree frog. *Immunogenetics* **69**, 165.

Kumar, S., Stecher, G. & Tamura, K. (2016). MEGA7: molecular evolutionary genetics analysis version 7.0 for bigger datasets. *Mol. Biol. Evol.* **33**, 1870.

Lal, M.M., Southgate, P.C., Jerry, D.R., Bosserelle, C. & Zenger, K.R. (2017). Swept away: ocean currents and seascape features influence genetic structure across the 18,000 Km Indo-Pacific distribution of a marine invertebrate, the black-lip pearl oyster *Pinctada margaritifera*. *BMC Genom.* **18**, 66.

Lebrón, J.A., Bennett, M.J., Vaughn, D.E., Chirino, A.J., Snow, P.M., Mintier, G.A., Feder, J.N. & Bjorkman, P.J. (1998). Crystal structure of the hemochromatosis protein HFE and characterization of its interaction with transferrin receptor. *Cell* **93**, 111.

Lewontin, R. & Krakauer, J. (1973). Distribution of gene frequency as a test of the theory of the selective neutrality of polymorphisms. *Genetics* **74**, 175.

Lillie, M., Grueber, C.E., Sutton, J.T., Howitt, R., Bishop, P.J., Gleeson, D. & Belov, K. (2015). Selection on MHC class II supertypes in the New Zealand endemic Hochstetter's frog. *BMC Evol. Biol.* **15**, 63.

Lipovich, L., Lynch, E.D., Lee, M.K. & King, M.C. (2001). A novel sodium bicarbonate cotransporter-like gene in an ancient duplicated region: SLC4A9 at 5q31. *Genome Biol* **2**, Research0011.

Luu, K., Bazin, E. & Blum, M.G. (2017). pcadapt: an R package to perform genome scans for selection based on principal component analysis. *Mol. Ecol. Resour.* **17**, 67.

Madsen, T. & Ujvari, B. (2006). MHC class I variation associates with parasite resistance and longevity in tropical pythons. *J. Evol. Biol.* **19**, 1973.

Maeshima, K., Morimatsu, K. & Horii, T. (1996). Purification and characterization of XRad51. 1 protein, *Xenopus* RAD51 homologue: recombinant XRad51. 1 promotes strand exchange reaction. *Genes Cells* **1**, 1057.

Matsumura, M., Fremont, D.H., Peterson, P.A. & Wilson, I.A. (1992). Emerging principles for the recognition of peptide antigens by MHC class I molecules. *Science* **257**, 927.

McFadden, M., Hobbs, R., Marantelli, G., Harlow, P., Banks, C. & Hunter, D. (2013). Captive management and breeding of the critically endangered southern corroboree frog

(*Pseudophryne corroboree*) (Moore 1953) at Taronga and Melbourne Zoos. *Amphib. Reptile Conserv.* **5**, 70.

Meyer, W., Seegers, U., Schnapper, A., Neuhaus, H., Himstedt, W. & Toepfer-Petersen, E. (2007). Possible antimicrobial defense by free sugars on the epidermal surface of aquatic vertebrates. *Aquat. Biol.* **1**, 167.

Morgan, M.J., Hunter, D., Pietsch, R., Osborne, W. & Keogh, J.S. (2008). Assessment of genetic diversity in the critically endangered Australian corroboree frogs, *Pseudophryne corroboree* and *Pseudophryne pengilleyi*, identifies four evolutionarily significant units for conservation. *Mol. Ecol.* **17**, 3448.

Narum, S.R., Buerkle, C.A., Davey, J.W., Miller, M.R. & Hohenlohe, P.A. (2013). Genotyping-by-sequencing in ecological and conservation genomics. *Mol. Ecol.* **22**, 2841.

Nemanic, M.K., Whitehead, J.S. & Elias, P.M. (1983). Alterations in membrane sugars during epidermal differentiation: visualization with lectins and role of glycosidases. *J. Histochem. Cytochem.* **31**, 887.

Novak, B. (2018). Advancing a new toolkit for conservation: from science to policy. *CRISPR J.* **1**, 11.

Petersen, B. (2017). Basics of genome editing technology and its application in livestock species. *Reprod. Domest. Anim.* **52**, 4.

Petersen, C., Fuzesi, L. & Hoyer-Fender, S. (1999). Outer dense fibre proteins from human sperm tail: molecular cloning and expression analyses of two cDNA transcripts encoding proteins of approximately 70 kDa. *Mol. Hum. Reprod.* **5**, 627.

Phillott, A.D., Grogan, L.F., Cashins, S.D., McDonald, K.R., Berger, L. & Skerratt, L.F. (2013). Chytridiomycosis and seasonal mortality of tropical stream-associated frogs 15 years after introduction of *Batrachochytrium dendrobatidis*. *Conserv. Biol.* **27**, 1058.

Pinheiro, J., Bates, D., DebRoy, S., Sarkar, D. & Team, R.C. (2009). *nlme: Linear and nonlinear mixed effects models*. R package version 3. Vienna: R foundation for statistical computing.

Poorten, T.J., Stice-Kishiyama, M.J., Briggs, C.J. & Rosenblum, E.B. (2016). Mountain yellow-legged frogs (*Rana muscosa*) did not produce detectable antibodies in immunization experiments with *Batrachochytrium dendrobatidis*. *J. Wildl. Dis.* **52**, 154.

Pritchard, J.K., Stephens, M. & Donnelly, P. (2000). Inference of population structure using multilocus genotype data. *Genetics* **155**, 945.

Ramsey, J.P., Reinert, L.K., Harper, L.K., Woodhams, D.C. & Rollins-Smith, L.A. (2010). Immune defenses against *Batrachochytrium dendrobatidis*, a fungus linked to global amphibian declines, in the South African clawed frog, *Xenopus laevis*. *Infect. Immun.* **78**, 3981.

Richmond, J.Q., Savage, A.E., Zamudio, K.R. & Rosenblum, E.B. (2009). Toward immunogenetic studies of amphibian chytridiomycosis: linking innate and acquired immunity. *Bioscience* **59**, 311.

Rocha, N. & Neefjes, J. (2008). MHC class II molecules on the move for successful antigen presentation. *EMBO J.* **27**, 1.

Rönnegård, L., McFarlane, S.E., Husby, A., Kawakami, T., Ellegren, H. & Qvarnström, A. (2016). Increasing the power of genome wide association studies in natural populations using repeated measures–evaluation and implementation. *Methods Ecol. Evol.* **7**, 792.

Rousset, F. (2008). GENEPOP'007: a complete re-implementation of the GENEPOP software for Windows and Linux. *Mol. Ecol. Resour.* **8**, 103.

Sandberg, M., Eriksson, L., Jonsson, J., Sjöström, M. & Wold, S. (1998). New chemical descriptors relevant for the design of biologically active peptides. A multivariate characterization of 87 amino acids. *J. Med. Chem.* **41**, 2481.

Savage, A.E. & Zamudio, K.R. (2011). MHC genotypes associate with resistance to a frog-killing fungus. *Proc. Natl Acad. Sci. USA* **108**, 16705.

Scheele, B.C., Hunter, D.A., Grogan, L.F., Berger, L., Kolby, J.E., McFadden, M.S., Marantelli, G., Skerratt, L.F. & Driscoll, D.A. (2014). Interventions for reducing extinction risk in chytridiomycosis-threatened amphibians. *Conserv. Biol.* **28**, 1195.

Scheele, B.C., Skerratt, L.F., Hunter, D.A., Banks, S.C., Pierson, J.C., Driscoll, D.A., Byrne, P.G. & Berger, L. (2017). Disease-associated change in an amphibian life-history trait. *Oecologia* **184**, 825–833.

Skerratt, L., Berger, L., Speare, R., Cashins, S., McDonald, K., Phillott, A., Hines, H. & Kenyon, N. (2007). Spread of chytridiomycosis has caused the rapid global decline and extinction of frogs. *EcoHealth* **4**, 125.

Skerratt, L.F., Mendez, D., McDonald, K.R., Garland, S., Livingstone, J., Berger, L. & Speare, R. (2011). Validation of diagnostic tests in wildlife: the case of chytridiomycosis in wild amphibians. *J. Herpetol.* **45**, 444.

Takashima, M., Hamamoto, M. & Nakase, T. (2000). Taxonomic significance of fucose in the class Urediniomycetes: distribution of fucose in cell wall and phylogeny of urediniomycetous yeasts. *Syst. Appl. Microbiol.* **23**, 63.

Teo, Y.Y., Fry, A.E., Clark, T.G., Tai, E.S. & Seielstad, M. (2007). On the usage of HWE for identifying genotyping errors. *Ann. Hum. Genet.* **71**, 701.

Therneau, T.M. (2015). A package for survival analysis in S. Version 2.38. Available at https://CRAN.R-project.org/package=survival

Van Prooyen, N., Henderson, C.A., Murray, D.H. & Sil, A. (2016). $CD103^{+}$ conventional dendritic cells are critical for TLR7/9-dependent host defense against *Histoplasma capsulatum*, an endemic fungal pathogen of humans. *PLoS Pathog.* **12**, e1005749.

Van Rooij, P., Martel, A., Haesebrouck, F. & Pasmans, F. (2015). Amphibian chytridiomycosis: a review with focus on fungus-host interactions. *Vet. Res.* **46**, 137.

Voyles, J., Young, S., Berger, L., Campbell, C., Voyles, W.F., Dinudom, A., Cook, D., Webb, R., Alford, R.A., Skerratt, L.F. & Speare, R. (2009). Pathogenesis of chytridiomycosis, a cause of catastrophic amphibian declines. *Science* **326**, 582.

Warr, G.W., Magor, K.E. & Higgins, D.A. (1995). IgY: clues to the origins of modern antibodies. *Immunol. Today* **16**, 392.

Wilson, D.J. & McVean, G. (2006). Estimating diversifying selection and functional constraint in the presence of recombination. *Genetics* **172**, 1411.

Wright, B., Willet, C.E., Hamede, R., Jones, M., Belov, K. & Wade, C.M. (2017). Variants in the host genome may inhibit tumour growth in devil facial tumours: evidence from genome-wide association. *Sci. Rep.* **7**, 423.

Yamamoto, T., Hikino, T., Nakayama, Y. & Abé, S.I. (1999). Newt RAD51: cloning of cDNA and analysis of gene expression during spermatogenesis. *Dev. Growth Differ.* **41**, 401.

Young, S., Whitehorn, P., Berger, L., Skerratt, L.F., Speare, R., Garland, S. & Webb, R. (2014). Defects in host immune function in tree frogs with chronic chytridiomycosis. *PLoS ONE* **9**, e107284.

Supporting information

Additional supporting information may be found online in the Supporting Information section at the end of the article.

Figure S1. Alignment of *Pseudophryne corroboree* major histocompatibility complex class IA amino acid sequences.
Figure S2. Comparison of ω across the *Pseudophryne corroboree* major histocompatibility complex class IA amino acid alignment.
Figure S3. Evolutionary relationships of major histocompatibility complex (MHC) class IA nucleotide sequences and MHC supertypes in *Pseudophryne corroboree* and other vertebrates.
Figure S4. Manhattan plots with $-\log_{10}$ *P*-values from the genome-wide association studies association with marker (single nucleotide polymorphisms) genotype for (a) days survived, (b) maximum infection load (GenABEL) and (c) infection load per week (RepeatABEL).
Figure S5. Clustering of *Pseudophryne corroboree* individuals using STRUCTURE for $K = 2$ and $K = 3$ clusters.
Table S1. Major histocompatibility complex class IA Sanger sequencing summary information.
Table S2. Major histocompatibility complex class IA allele frequencies.
Table S3. Major histocompatibility complex class IA supertype frequencies.
Table S4. Results of generalized least squares for major histocompatibility complex class IA alleles associated maximum infection load.
Table S5. Results of generalized least squares for major histocompatibility complex class IA alleles associated with days survived.
Table S6. Results of generalized least squares for major histocompatibility complex class IA supertypes associated with maximum infection load.
Table S7. Results of generalized least squares for major histocompatibility complex class IA supertypes associated with days survived.
Table S8. Descriptive information on the top 10 single nucleotide polymorphisms for the genome-wide association studies models.
Table S9. Corroboree frog population genetic differentiation (F_{ST}) values.
Table S10. Corroboree frog single nucleotide polymorphism outlier frequency by population.
Data S1. Supplementary tables and figures.
Data S2. Supplementary Materials and Methods.